



Chinese Pharmaceutical Association  
Institute of Materia Medica, Chinese Academy of Medical Sciences

Acta Pharmaceutica Sinica B

[www.elsevier.com/locate/apsb](http://www.elsevier.com/locate/apsb)  
[www.sciencedirect.com](http://www.sciencedirect.com)



ORIGINAL ARTICLE

# Molecular insights into AabZIP1-mediated regulation on artemisinin biosynthesis and drought tolerance in *Artemisia annua*



Guoping Shu<sup>a</sup>, Yueli Tang<sup>a</sup>, Mingyuan Yuan<sup>a</sup>, Ning Wei<sup>a</sup>,  
Fangyuan Zhang<sup>a</sup>, Chunxian Yang<sup>a</sup>, Xiaozhong Lan<sup>b</sup>, Min Chen<sup>c</sup>,  
Kexuan Tang<sup>a</sup>, Lien Xiang<sup>d</sup>, Zhihua Liao<sup>a,\*</sup>

<sup>a</sup>Key Laboratory of Eco-environments in Three Gorges Reservoir Region (Ministry of Education), Chongqing Engineering Research Centre for Sweet Potato, SWU-TAAHC Medicinal Plant Joint R&D Centre, School of Life Sciences, Southwest University, Chongqing 400715, China

<sup>b</sup>TAAHC-SWU Medicinal Plant Joint R&D Centre, Xizang Agricultural and Husbandry College, Nyingchi 860000, China

<sup>c</sup>College of Pharmaceutical Sciences, Southwest University, Chongqing 400715, China

<sup>d</sup>College of Environmental Science and Engineering, China West Normal University, Nanchong 637009, China

Received 13 June 2021; received in revised form 30 August 2021; accepted 19 September 2021

## KEY WORDS

*Artemisia annua*;  
AabZIP1;  
AaMYC2;  
Artemisinin biosynthesis;  
Drought tolerance;  
Wax biosynthesis

**Abstract** *Artemisia annua* is the main natural source of artemisinin production. In *A. annua*, extended drought stress severely reduces its biomass and artemisinin production while short-term water-withholding or abscisic acid (ABA) treatment can increase artemisinin biosynthesis. ABA-responsive transcription factor AabZIP1 and JA signaling AaMYC2 have been shown in separate studies to promote artemisinin production by targeting several artemisinin biosynthesis genes. Here, we found AabZIP1 promote the expression of multiple artemisinin biosynthesis genes including *AaDBR2* and *AaALDH1*, which AabZIP1 does not directly activate. Subsequently, it was found that AabZIP1 up-regulates *AaMYC2* expression through direct binding to its promoter, and that AaMYC2 binds to the promoter of *AaALDH1* to activate its transcription. In addition, AabZIP1 directly transactivates wax biosynthesis genes *AaCER1* and *AaCYP86A1*. The biosynthesis of artemisinin and cuticular wax and the tolerance of drought stress were significantly increased by *AabZIP1* overexpression, whereas they were significantly decreased in RNAi-*AabZIP1* plants. Collectively, we have uncovered the AabZIP1-AaMYC2 transcriptional module as a point of cross-talk between ABA and JA signaling in artemisinin biosynthesis, which may have

\*Corresponding author.

E-mail address: [zhiliao@swu.edu.cn](mailto:zhiliao@swu.edu.cn) (Zhihua Liao).

Peer review under responsibility of Chinese Pharmaceutical Association and Institute of Materia Medica, Chinese Academy of Medical Sciences.

<https://doi.org/10.1016/j.apsb.2021.09.026>

2211-3835 © 2022 Chinese Pharmaceutical Association and Institute of Materia Medica, Chinese Academy of Medical Sciences. Production and hosting by Elsevier B.V. This is an open access article under the CC BY-NC-ND license (<http://creativecommons.org/licenses/by-nc-nd/4.0/>).

general implications. We have also identified AabZIP1 as a promising candidate gene for the development of *A. annua* plants with high artemisinin content and drought tolerance in metabolic engineering breeding.

© 2022 Chinese Pharmaceutical Association and Institute of Materia Medica, Chinese Academy of Medical Sciences. Production and hosting by Elsevier B.V. This is an open access article under the CC BY-NC-ND license (<http://creativecommons.org/licenses/by-nc-nd/4.0/>).

## 1. Introduction

*Artemisia annua*, a traditional Chinese medicinal plant, is well-known for producing anti-malarial artemisinin. Apart from its irreplaceable function in malaria treatment, artemisinin also shows great potential in the treatment of lupus erythematosus<sup>1</sup>, diabetes<sup>2</sup>, tuberculosis<sup>3</sup> and malignant tumors<sup>4</sup>. With the discovery of new uses of artemisinin, the demand for the chemical is growing worldwide. Artemisinin can be synthesized chemically, and its precursors, artemisinic acid and dihydroartemisinic acid, have also been successfully obtained in *Saccharomyces cerevisiae* through recombinant microbial pathways<sup>5,6</sup>, which can realize semi-synthetic production of artemisinin. Unfortunately, these methods are difficult to use for poor Southeast Asian and African countries due to the high cost, and therefore can not be used as a staple method for production of artemisinin. Therefore, *A. annua* plant is still the primary source of commercial production of artemisinin now and for a long time in the future<sup>7</sup>. Thus it is important to develop *A. annua* germplasm resources with high artemisinin content and strong tolerance to environmental stress.

Drought is one of the main environmental factors affecting plant growth and crop yield<sup>8</sup>, as the metabolism and productivity are decreased in wheat<sup>9</sup>, rice<sup>10</sup> and maize<sup>11</sup> under extended drought stress. For *A. annua*, previous research revealed that, while short-term water shortage could increase artemisinin production, long-term drought stress caused a decline in the levels of many metabolites (including artemisinin) and biomass, and induced a decrease in the density and size of glandular trichomes where artemisinin is produced and stored<sup>12,13</sup>. To cope with drought stress, plants have evolved many sophisticated adaptive mechanisms to modify relevant physiological and cellular traits<sup>14,15</sup>, such as increasing the accumulation of cuticular wax. Plant organs are covered with a layer of cuticular wax, which acts as a protective barrier to prevent excessive water loss across the primary surface, thereby making plants more tolerant to drought conditions<sup>16,17</sup>. Cuticular waxes are mainly composed of a series of very long-chain aliphatic compounds, including acyl esters (wax esters), alkanes, aldehydes, fatty acids, alcohols and ketones<sup>18,19</sup>. Multiple types of enzymes involved in wax biosynthesis have been reported, such as fatty acid hydroxylase (CER)<sup>20</sup>, ketoacyl-CoA synthase (KCS)<sup>21</sup> and formate dehydrogenase (FDH)<sup>22</sup>, etc. Studies have shown that the expression of genes encoding these enzymes is significantly increased under drought stress<sup>16,23,24</sup>, primarily through the activation by stress-induced transcription factors (TFs) in plants<sup>25</sup>. Under drought conditions, drought- and abscisic acid (ABA)-inducible MYB94 and MYB96 enhanced the expression of wax biosynthesis genes, such as *KCS* and *CER*, by directly binding to their promoters in *Arabidopsis*<sup>16,26</sup>. In addition, the *Arabidopsis* AP2/DREB transcription factor RAP2.4, which was induced by drought and ABA treatment, directly activated the expression of *CER* and *KCS* genes involved in wax biosynthesis in response to drought stress<sup>27</sup>.

Moreover, SIMYB31 and WOOLLY, whose expression was upregulated by drought and ABA treatment, promoted cuticular wax biosynthesis in response to drought stress in tomato<sup>28</sup>. In *A. annua*, AaTAR1, AaMIXTA1 and AaHD8 have been reported to promote cuticle wax biosynthesis by positively regulating the transcription of wax-related genes<sup>29–31</sup>, including *AaCER1*, *AaCYP86A1*, *AaKCS5* and *AaFDH*, etc. However, up to now, little is known about the molecular link between drought stress and cuticular wax biosynthesis in *A. annua*.

bZIP TFs have been reported to play important roles not only in regulating the biosynthesis of secondary metabolites, but also in response to abiotic stress such as drought<sup>32–35</sup>. For example, drought or ABA treatments induced the transcription of AabZIP1 in *A. annua*<sup>36</sup>, but the specific roles of AabZIP1 in drought response remains unclear. AabZIP1, a homologue to *Arabidopsis* AtABF1<sup>36</sup> involved in ABA signaling pathway, regulates artemisinin biosynthesis in *A. annua* by directly activating the transcription of two artemisinin biosynthesis genes, *AaADS* and *AaCYP71AV1*, through binding to their promoters<sup>36</sup>. But it is not known whether AabZIP1 can regulate the transcription of *AaDBR2* and *AaALDH1*, another two genes involved in artemisinin biosynthesis. Therefore, significant gaps remain in our understanding of the function and the regulatory mode of AabZIP1 in artemisinin biosynthesis as well as in drought tolerance. *A. annua* is the main natural source of artemisinin production, extended drought stress reduces its biomass and artemisinin production while short-term drought stress can increase artemisinin biosynthesis<sup>12,13</sup>. Therefore, studying the potential interaction between drought stress and artemisinin biosynthesis in *A. annua* can provide the theoretical basis for the development of *A. annua* germplasm resources with strong drought tolerance and high yield of artemisinin.

Jasmonic acid (JA) also plays an important role in regulating artemisinin biosynthesis<sup>37</sup>. In *A. annua*, AaMYC2, a key JA pathway TF, positively regulates artemisinin biosynthesis in part by directly activating the expression of artemisinin biosynthesis genes *AaCYP71AV1* and *AaDBR2*<sup>38</sup>. But it is not known whether AaMYC2 can also regulate *AaADS* and *AaALDH1*, another two genes involved in artemisinin biosynthesis. In addition, the expression of *AaMYC2* can also be induced by ABA treatment<sup>38</sup> as in the case of *Arabidopsis*<sup>39,40</sup>. However the mechanism of ABA-induced transcriptional upregulation of MYC2 has not been clearly defined either in *A. annua*.

In this study, we expanded the role of AabZIP1 in *A. annua*. It was found that AabZIP1 can directly activate AaMYC2 expression by binding to its promoter, and AaMYC2 in turn activates the expression of *AaALDH1*, which results in increased artemisinin production. These new results showed that AabZIP1 not only activates several artemisinin biosynthesis genes directly, but also play a role in invoking the JA pathway to coordinately enhance the production of artemisinin. In addition, it was found that the *AabZIP1*-overexpressing *A. annua* plants exhibited higher drought

tolerance, due to increased cuticular wax accumulation. It is revealed that AabZIP1 directly activates the expression of two wax biosynthesis genes (*AaCER1* and *AaCYP86A1*) through binding to their promoters, thus promoting cuticular wax accumulation and leading to higher resistance to drought stress. These results expanded the knowledge for regulatory network in artemisinin biosynthesis and response to environmental stress.

## 2. Materials and methods

### 2.1. Plant cultivation and stress treatment

Seeds were harvested from wild-type *A. annua* grown in the experimental field of Southwest University (Chongqing, China) for this study. These seeds were surface-sterilized with 15% sodium hypochlorite solution for 20 min, and then washed three times with sterile water. Subsequently, seeds were germinated on 1/2 MS solid medium at  $23 \pm 2^\circ\text{C}$  under a light period of 16-h light/8-h dark. All seedlings were grown in pots with organic substrates in an artificial climate room at  $23 \pm 2^\circ\text{C}$  under a light period of 16-h light/8-h dark. *Nicotiana benthamiana* seeds were sown directly in soil and their growth conditions are consistent with that of *A. annua* plants. Tobacco plants grown for 4 weeks old were used for dual-luciferase assays.

### 2.2. Drought and ABA treatments

For drought-induced genes expression analysis shown in Fig. 1, drought stress was performed as described previously<sup>36,41,42</sup>, by removing the 30-day-old wild-type (WT) plants from water-saturated pots and placing the intact plants on dry filter papers, while the control plants were put on water-saturated filter paper. Leaves were collected at 0, 3, 6, 12 and 24 h after the treatment, and then were frozen immediately in liquid nitrogen. For drought tolerance analysis (Fig. 2), WT, transgenic OE-*AabZIP1* (OE-2) and RNAi-*AabZIP1* (Ri-1) seedlings were grown in the pots for 45 days under normal conditions. Then plants were water-withheld for 12 days, when plants started to show signs of slight water deficiency, and was regarded as the initiation of the drought stress

treatment. Plants were photographed every two days. At Day 20 of water withholding, pots were re-watered to re-hydrate the plants, and photographs were taken after 4 days of recovery.

For ABA treatment, 30 days old intact WT *A. annua* plants were treated with 10  $\mu\text{mol/L}$  exogenous ABA solution containing 0.5% ethanol, or 0.5% ethanol solution as the mock treatment. All leaves of *A. annua* plants at 0, 3, 6, 12 and 24 h after exogenous ABA and mock treatment were collected, and frozen immediately in liquid nitrogen for subsequent experiments.

### 2.3. *Artemisia annua* plant transformation

For obtaining the reconstruction plasmid of pHB-AabZIP1, *AabZIP1* was inserted into pHB plasmid driven by double CaMV 35S promoter through *Bam*H1 and *Pst*I sites. Meanwhile, a 351-bp fragment of *AabZIP1* coding sequence was selected to construct the RNAi vector, pBIN19-AabZIP1. The constructs were separately transferred into *Artemisia tumefaciens* strain EHA105 to form engineering strains. These strains were grown on YEP solid medium containing related antibiotics for 48 h. Subsequently, positive monoclonal strain was inoculated into YEP liquid medium containing related antibiotics for culture until the OD<sub>600</sub> value of the medium reaches 0.6. The supernatant was discarded after centrifugation, and then resuspended in the 1/2 MS liquid to OD<sub>600</sub> = 0.3–0.5, 200 rpm shaking culture at  $28^\circ\text{C}$  for 30 min. Cultured engineered strains were used to transform *A. annua* via *Agrobacterium*-mediated transformation as described previously<sup>38</sup>. After that, the obtained seedlings were transplanted into pots with organic substrates and cultured in an artificial climate room at  $23 \pm 2^\circ\text{C}$  under a light period of 16-h light/8-h dark.

### 2.4. Quantitative real-time PCR (qRT-PCR)

The qRT-PCR was performed to analyze all genes expression in this study. The total RNA of these samples from wide-type and transgenic plants were extracted using the total plant RNA Extract Kit (Tiangen, China), and then reversely transcribed into cDNA using FastKing RT Kit (with DNase) FastKing cDNA (Tiangen, China). Subsequently, the cDNA was used as the template to

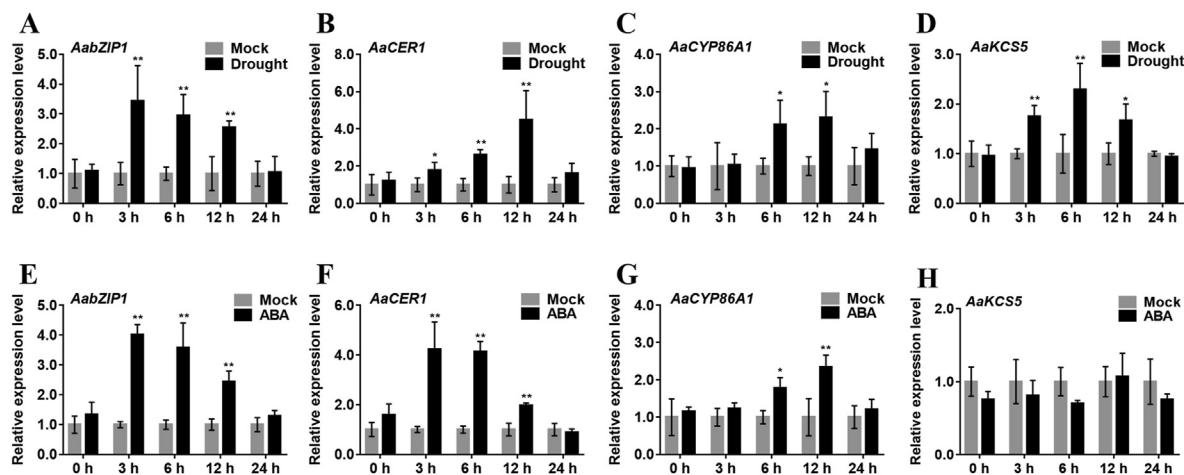


**Figure 1** Expression analysis of *AabZIP1* and wax biosynthesis genes in the leaves of 30-day-old wild-type *A. annua* under drought and abscisic acid (ABA) treatments. (A–D) Relative expression levels of *AabZIP1*, *AaCER1*, *AaCYP86A1* and *AaKCS5* in plants subjected to drought for 0–24 h, normally watered plants are shown as mock. (E–H) Relative expression levels of *AabZIP1*, *AaCER1*, *AaCYP86A1* and *AaKCS5* in plants under 10  $\mu\text{mol/L}$  exogenous ABA treatment for 0–24 h, 0.5% ethanol solution was used as mock treatment. The data represents the means  $\pm$  SD ( $n = 3$ ), \* $P < 0.05$ , \*\* $P < 0.01$  in Student's *t*-test.

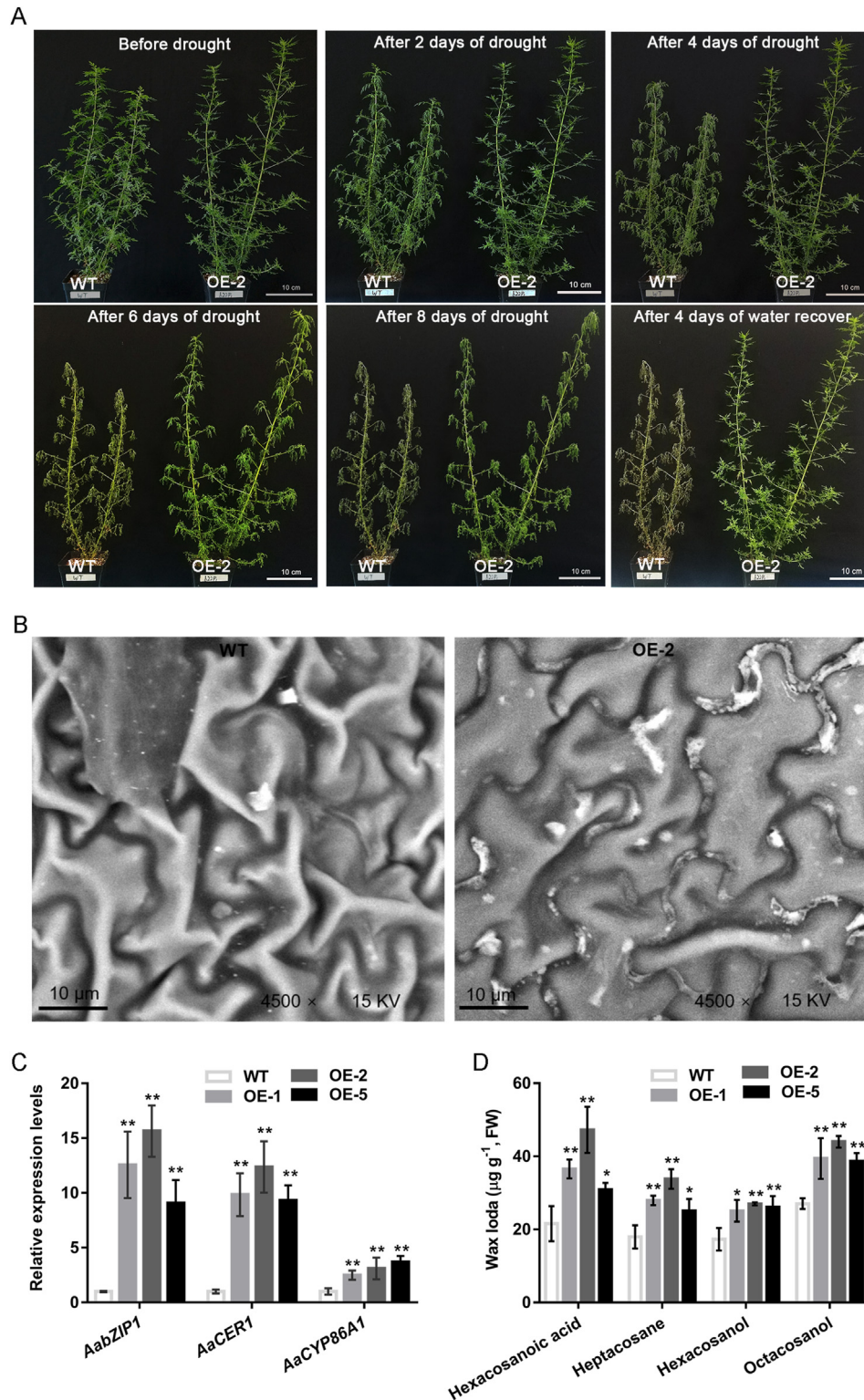


**Figure 2** Response of wild-type (WT) and *AabZIP1*-overexpression (OE-*AabZIP1*) *A. annua* to drought stress and analysis of cuticular wax in *A. annua* leaves. (A) Representative pictures show the phenotypes of 57-day-old WT and OE-2 transgenic *A. annua* plants before drought stress, after drought stress (2, 4, 6 and 8 days) and after 4 day of water recovery while growing in soil. Bars represent 10 cm in all images. (B) SEM images of adaxial side from leaf 7 of 57-day-old WT and OE-2 transgenic *A. annua* plants, the leaf surface of OE-2 line is covered with wax crystals and is smooth, whereas WT leaf surface shows little wax deposition. The bars represent 10  $\mu\text{m}$  in all images. (C) Expression levels of *AabZIP1*, *AaCER1* and *AaCYP86A1* in leaves of WT and OE-*AabZIP1* transgenic *A. annua*. (D) The contents of cuticular wax components in leaves 6, 7 and 8 from the main stem of WT and OE-*AabZIP1* transgenic *A. annua* were analyzed by GC-MS. OE-1, OE-2 and OE-5 are independent lines of *AabZIP1*-overexpressing *A. annua* plants. The data represents the means  $\pm$  SD ( $n = 3$ ), \* $P < 0.05$ , \*\* $P < 0.01$  in Student's *t*-test.

detect the expression levels of *AabZIP1* and wax biosynthesis genes by qRT-PCR experiment. The qRT-PCR amplification conditions were 95 °C for 3 min, followed by 40 cycles of 95 °C for 10 s, 56 °C for 20 s, and 72 °C for 20 s. The  $\beta$ -actin of *A. annua* was used as the reference gene in this study<sup>43</sup>. The relative expression levels of target genes were calculated using the  $2^{-\Delta\Delta CT}$  method<sup>44</sup>. The primer sequences in qRT-PCR were listed in Supporting Information Table S1.

### 2.5. Scanning electron microscopy (SEM)

To observe the accumulation of cuticular waxes, scanning electron microscopy (SEM) was carried out using methods reported previously<sup>30</sup>. Leaf-7 (the 7th leaf below the meristem) from 8 weeks old transgenic and wild-type *A. annua* plants were fixed in 2.5% glutaraldehyde fixative at room temperature for 5 h, respectively. The samples were washed three times with 0.1 mol/L phosphate buffer (pH 7.0) for 10 min each time, dehydrated for 10 min through a series of alcohol concentration gradient (30%, 40%, 50%, 60%, 70%, 80%, 95%), and then samples were dehydrated three times with 100% ethanol for 5 min each time and dried in a critical point drying device (Leica 011206, Germany). The prepared samples were coated with 20 Å gold particles, and the observation of cuticular waxes was fulfilled by SEM (Phenom-World BV, Phenom Pro010102).

### 2.6. Plant leaf cuticular waxes extraction and GC-MS analysis

The cuticular waxes of *A. annua* leaves were analyzed by GC-MS as described before with some modifications<sup>29–31</sup>. A total of 0.5 g fresh leaves from leaves 6, 7 and 8 from the main stem of 8 weeks old transgenic and wild-type *A. annua* were collected and thoroughly extracted with 5 mL chloroform for 3 min at room temperature. The supernatant was filtered through a 0.22  $\mu$ m-size filters and then the solvents were lyophilized through a gentle stream of nitrogen. The resulting residues were dissolved with 500  $\mu$ L chloroform, and then these mixtures were transferred into 1.5 mL tube and dried again under a gentle stream of nitrogen. The resulting residues were derivatized with a mixture of 100  $\mu$ L pyridine and 100  $\mu$ L bis-*N,N*-(trimethylsilyl) trifluoroacetamide for 1 h at 70 °C and then 1000  $\mu$ L *n*-heptane containing tricosane (as internal standard) was added to dilute the solution. The solution was centrifuged at 12,000 rpm for 5 min. The supernatant was analyzed by gas chromatography-mass spectrometry (GC-MS-QP2010 Ultra; Shimadzu) with the temperature program: initial temperature of 70 °C (1 min hold), increase to 160 °C at 10 °C/min, and then ramp to 240 °C at 5 °C/min. Finally, increase to 280 °C at 20 °C/min (17 min hold). Helium was used as a carrier gas and 1  $\mu$ L sample was injected in split mode; split rate, 2:1; ion source temperature, 230 °C; ionization voltage, 70 eV with scanning from *m/z* 33 to 500. Qualitative analysis of wax components was fulfilled by comparing with NIST (National Institute of Standards and Technology) database and Wiley libraries. Single compounds were quantified against the internal standards by automatically integrating the peak areas.

### 2.7. Measurement of artemisinin and dihydroartemisinic acid

For artemisinin and dihydroartemisinic acid analyses, all mature leaves of 3 months old transgenic and wild-type *A. annua* plants were collected and drying at 50 °C, and then used for the detection

of artemisinin and dihydroartemisinic acid contents using HPLC as described previously<sup>45</sup>. At least three replications were completed. Standard samples of artemisinin and dihydroartemisinic acid were purchased from Sigma-Aldrich in this study.

### 2.8. Dual-LUC assay

Dual-LUC assays were performed using methods reported previously<sup>36</sup>. The promoter sequences of *AaCER1* (MF144191), *AaCYP86A1* (MF144190), *AaADS* (DQ448294), *AaDBR2* (KC118523.1), *AaALDH1* (KC118525.1) and *AaMYC2* (Supporting Information Fig. S4) were cloned and inserted into pGreenII 0800-LUC plasmid to generate pAaCER1:LUC, pAaCYP86A1:LUC, pAaADS:LUC, pAaDBR2:LUC, pAaALDH1:LUC and pAaMYC2:LUC constructs as reporter vectors, respectively. Subsequently, these reporter vectors were transferred into *A. tumefaciens* strain GV3101 together with the pSoup plasmid. The *AabZIP1* and *AaMYC2* were inserted into the pHB plasmid driven by double CaMV 35S promoter as the effector vector and also transferred into *A. tumefaciens* strain GV3101. Meanwhile, the pHB-YFP (a yellow fluorescent protein construct driven by double 35S promoter) plasmid was transferred into GV3101 as a negative control. All engineering and control strains were inoculated into YEP liquid select medium and cultured overnight at 28 °C. The agrobacterium cells were collected by centrifuge at 4500 rpm for 10 min and resuspended in the MS liquid to OD<sub>600</sub> = 0.6  $\pm$  0.05. The acetosyringone (As, 100 mmol/L, 1:500, v/v) and 2-(*N*-morpholino) ethanesulfonic acid (MES, 0.5 mol/L (pH = 5.7), 1:50, v/v) were added to the resuspension and then were injected into tobacco leaves after being placed for 4 h at room temperature. Tobacco plants injected with agrobacterium cells were exposed to weak light for 48 h. A small piece of tobacco leaves (about 2 cm in diameter) was collected to 1.5 mL tube and immediately was ground in liquid nitrogen. The relative LUC/REN activity was tested using Dual-Luciferase® Reporter Assay System 10-Pack (Promega) according to the manufacturer's instructions.

### 2.9. Yeast one-hybrid assay

To investigate how *AabZIP1* regulates the expression of *AaCER1*, *AaCYP86A1* and *AaMYC2*, yeast one-hybrid assays were fulfilled. The *AabZIP1* coding sequence was inserted into pB42AD plasmid containing the GAL4 activation domain (AD) through *EcoRI* and *XhoI* sites to generate pB42AD-*AabZIP1* constructs as the prey. The 45 bp fragments containing one ABRE *cis*-element from *AaCER1*, *AaCYP86A1* and *AaMYC2* promoters, named pAaCER1-R1 (−987 to −943), pAaCER1-R2 (−440 to −396), pAaCER1-R3 (−147 to −103), pAaCYP86A1-R1 (−1707 to −1663), pAaCYP86A1-R2 (−1676 to −1632), pAaMYC2-R1 (−1034 to −1027), pAaMYC2-R2 (−998 to −982), pAaMYC2-R3 (−678 to −664) and pAaMYC2-R4 (−412 to −393), were inserted into pLacZ plasmids through *KpnI* and *XhoI* sites as the bait, respectively. The pB42AD-*AabZIP1* plasmid was co-transformed into yeast strain EGY48 with the above bait constructs, respectively. Similarly, the 45 bp fragments containing one G-box element from *AaADS* and *AaALDH1* promoters, pAaADS-G1 (−1384 to −1339), pAaADS-G2 (−474 to −429), pAaALDH1-G1 (−987 to −943) and pAaALDH1-G2 (−440 to −396), were inserted into pLacZ plasmids as the bait, respectively. The pB42AD-*AaMYC2* plasmid was co-transformed into yeast strain EGY48

with the above bait constructs, respectively. The yeast cells were grown on SD-Ura-Trp selective medium for 48 h at 30 °C. All independent yeast cells were shifted into SD-Ura-Trp liquid medium and cultured overnight at 30 °C, and then these cells were collected by microcentrifugation and resuspended in 100  $\mu$ L sterile water. Resuspended cells were grown on SD-Ura-Trp medium with 5-bromo-4-chloro-3-indolyl-*b*-D-galactopyranoside (X-gal) for 24–48 h at 30 °C. The empty pB42AD and pLacZ plasmids were used as negative controls. Five independent biological replicates were implemented for each experiment in this study. All sequences are listed in [Supporting Information Table S2](#).

### 2.10. Electrophoretic mobility shift assay

The *AabZIP1* and *AaMYC2* coding regions were inserted into pEGX-6P-1 plasmid through *EcoRI* and *XhoI* sites to generate *AabZIP1*- and *AaMYC2*-pEGX-6P-1 constructs respectively, and then transformed into *Escherichia coli* strain BL21 (DE3) for expression to obtain recombinant protein. The expression of fusion proteins was induced in DE3 cells by adding 0.5 mmol/L IPTG into LB liquid medium for 16 h at 18 °C. Subsequently, the DE3 cells were collected by centrifuge and disrupted. The supernatant was filtered to purify the *AabZIP1*- and *AaMYC2*-GST proteins using BeyoGold™ GST-tag Purification Resin (Beyotime Biotech Co.). The biotin-labeled 45 bp fragments containing ABRE *cis*-element from promoters of *AaCER1*, *AaCYP86A1* and *AaMYC2* respectively, and fragments containing G-box element from *AaALDH1* promoter, were synthesized as the probe by Invitrogen (Guangzhou, China). Two single-stranded DNA fragments were incubated for 5 min at 98 °C. Subsequently were  $-0.1$  °C per cycle from 98 to 25 °C, and then for 3 min at 25 °C to obtain an annealing product. EMSA was performed using the LightShift Chemiluminescent EMSA Kit (Beyotime Biotech Co.) according to the manufacturer's instructions. The GST protein was used as the negative control. All probe sequences are listed in [Supporting Information Table S3](#).

## 3. Results

### 3.1. Drought stress and ABA treatment induced the expression of *AabZIP1* and wax biosynthesis genes

To investigate the role of *AabZIP1* in drought and ABA response in *A. annua*, wild type plants were subjected to drought stress or ABA treatment as described in Material and Methods. qPCR analysis showed that *AabZIP1* expression was significantly and rapidly upregulated under drought stress or ABA treatment ([Fig. 1A](#) and [E](#)). In both cases the expression levels of *AabZIP1* were induced as early as 3 h after the treatments, and were largely sustained to 12 h, then began to decline. This result was consistent with the previous report<sup>36</sup>, further indicating that *AabZIP1* is involved in drought and ABA response in *A. annua*.

Several studies have shown that the expression of genes involved in wax biosynthesis is significantly increased under drought stress<sup>16,23</sup>. In this study, it was found that two wax biosynthesis genes, *AaCER1* and *AaCYP86A1*, were markedly induced under drought stress or ABA treatment, and the highest expression levels of *AaCER1* and *AaCYP86A1* were detected at 6 or 12 h after drought stress and ABA treatment ([Fig. 1](#)). These

results suggest that drought stress and ABA treatment can induce the expression of wax biosynthesis genes in *A. annua*.

### 3.2. *AabZIP1* promotes tolerance to drought stress and cuticular wax accumulation in *A. annua*

To further explore the function of *AabZIP1* in drought response in *A. annua*, transgenic plants overexpressing and suppressing *AabZIP1* were respectively generated ([Supporting Information Fig. S1](#)). qRT-PCR analysis showed the transcription level of *AabZIP1* was dramatically enhanced in *AabZIP1*-overexpression (OE-*AabZIP1*) transgenic *A. annua* plants by 9.05–15.64 times, compared to that in wild-type ([Fig. 2C](#)). Notably, the expression levels of *AaCER1* and *AaCYP86A1* were also significantly increased by about 9.3–12.4 and 2.5–4.0 times, respectively, in the three OE-*AabZIP1* lines when compared with the wide-type plants ([Fig. 2C](#)). In the RNAi transgenic lines, the transcript levels of *AabZIP1* were decreased by 40%–87%, compared with the control level, whereas the expression of *AaCER1* and *AaCYP86A1* were 51%–83% and 34%–65% lower, respectively ([Supporting Information Fig. S2C](#)). For *AaKCS5* and *AaFDH*, overexpression or suppression of *AabZIP1* did not significantly alter their transcription levels ([Supporting Information Fig. S3](#)). To investigate whether *AabZIP1* conferred the drought resistance in *A. annua* plants, the OE-*AabZIP1* (OE-2) and wild-type *A. annua* plants were subjected to drought tolerance test. After 12 days of the last watering, plants were considered under drought stress, and were monitored and photographed as day-0 ([Fig. 2A](#)). After 2 days of drought stress, wild-type *A. annua* leaves exhibited slight wilting, while the leaves of the OE-2 *A. annua* maintained flourishing. After 4 days of drought stress, wild-type leaves exhibited moderate wilting, while the leaves of OE-2 plants remained green and flourishing. After 6 and 8 days, wild-type plants were severely withered, while OE-2 plants showed only moderate wilting. Plants were re-watered at this point (day-8 of draught stress), and after 4 days of re-hydration, the OE-2 plants recovered to normal condition, while the wild-type plants failed to recover and died from severe water deficiency. By contrast, the Ri-1 plants exhibited significantly lower drought tolerance than the wild-type plants ([Fig. S2A](#)).

The morphology of cuticular waxes on the transgenic and wild-type *A. annua* leaves was examined by SEM. As shown in [Fig. 2B](#), wax crystals deposition was observed in OE-2 leaves, compared with wild-type plants. By contrast, the Ri-1 plants exhibited much less wax deposition than the wild-type plants ([Fig. S2B](#)). Moreover, the contents of cuticular waxes in transgenic and wild-type plants were analyzed by GC–MS, OE-*AabZIP1* transgenic lines produced cuticular wax compounds at significantly higher levels than wild-type plants ([Fig. 2D](#)). Compared with wild-type plants, the hexacosanoic acid product was increased by 43%–119%, heptacosane product was increased by 39%–88%, hexacosanol product was increased by 45%–56%, octacosanol product was increased by 43%–63% in the three transgenic lines ([Fig. 2D](#)). By contrast, in the RNAi lines, the production of hexacosanoic acid, heptacosane, hexacosanol, and octacosanol were decreased by 28%–47%, 33%–71%, 30%–84% and 65%–93%, respectively, compared with the wild type ([Fig. S2D](#)). The above results indicate that *AabZIP1* promotes the accumulation of cuticular wax, which would contribute to the enhanced drought tolerance in the OE-*AabZIP1* transgenic *A. annua* plants.

### 3.3. *AabZIP1* transcriptionally activates wax biosynthesis genes *AaCER1* and *AaCYP86A1* by binding to their promoters

To further study how *AabZIP1* regulates the expression of wax biosynthesis genes in *A. annua*, dual-LUC assays were performed. The promoter sequences of *AaCER1* (2040 bp) and *AaCYP86A1* (1604 bp) were used to drive the reporter gene in pAaCER1:LUC and pAaCYP86A1:LUC vectors, respectively, while the pHB-YFP (yellow fluorescent protein) plasmid was used as a negative control. When *AabZIP1*-YFP was co-expressed in *N. benthamiana* leaves, the promoter activities of *AaCER1* and *AaCYP86A1* were significantly increased, with the LUC/REN value of pAaCER1:LUC and pAaCYP86A1:LUC increased 7.4- and 2.1-fold than the YFP control (Fig. 3B), respectively. The result indicated *AabZIP1* can significantly enhance transcriptional activity of *AaCER1* and *AaCYP86A1* promoters in tobacco leaves.

It was previously reported that bZIP TFs can directly bind to ABRE (ACGTG) *cis*-elements in the target gene promoters<sup>36</sup>. Since multiple ABRE *cis*-elements exist in *AaCER1* and *AaCYP86A1* promoters (Fig. 3C and D), we evaluate whether *AabZIP1* can directly bind to these ABRE *cis*-elements by yeast one-hybrid (Y1H) assay. As shown in Fig. 3E and F, the results indicated that *AabZIP1* can directly bind to pAaCER1-R2 and pAaCYP86A1-R1 ABRE-containing fragments, but not the pAaCER1-R1, pAaCER1-R3 and pAaCYP86A1-R2 fragments. When the ABRE *cis*-elements in the pAaCER1-R2 and pAaCYP86A1-R1 fragments were mutated to the TTTTG sequences resulting in pAaCER1-mR2 and pAaCYP86A1-mR1, respectively, the binding signals of *AabZIP1* and pAaCER1-mR2 and pAaCYP86A1-mR1 were markedly weakened or disappeared, validating the specificity of the binding (Fig. 3E and F).

Next, to further confirm the binding of *AabZIP1* to ABRE-containing pAaCER1-R2 and pAaCYP86A1-R1 fragments, EMSAs were conducted. The 45-bp fragments containing ABRE *cis*-elements from pAaCER1-R2 and pAaCYP86A1-R1 were used as probes. The GST-*AabZIP1* protein was expressed and purified from *E. coli* and GST protein was used as a negative control. Different amounts of unlabeled probes served as competitors to confirm the DNA binding specificity. The results showed that *AabZIP1* can bind to the pAaCER1-R2 and pAaCYP86A1-R1 fragments *in vitro*, as indicated by the shift of the labeled probes (Fig. 3G and H). Moreover, *AabZIP1* bound to the ABRE *cis*-element were markedly weakened and by unlabeled competitor probes in a concentration-dependent manner. Taken together, these results demonstrate that *AabZIP1* enhances *AaCER1* and *AaCYP86A1* transcription most likely by directly binding to the specific ABRE motifs in their promoters.

### 3.4. *AabZIP1* enhanced the transcription of *AaDBR2* and *AaALDH1* by directly activating *AaMYC2* expression

It has been established that *AabZIP1* mediates ABA-induced artemisinin biosynthesis in part by directly activating the transcription of *AaADS* and *AaCYP71AV1*<sup>36</sup>. Artemisinin biosynthesis also requires two downstream enzymes encoded by *AaDBR2* and *AaALDH1*. In this study, we examined the expression levels of all four genes involved in artemisinin biosynthesis in transgenic and wild-type plants. qPCR results showed the expression levels of *AaDBR2* and *AaALDH1*, in addition to *AaADS* and *AaCYP71AV1*, were significantly increased in OE-*AabZIP1* lines compared to that in wild-type plants (Fig. 4A). By contrast, the expression levels of *AaADS*, *AaCYP71AV1*, *AaDBR2* and *AaALDH1* were

significantly suppressed in the RNAi-*AabZIP1* lines (Fig. S4A). Furthermore, compared with the wild-type, the artemisinin and dihydroartemisinic acid contents were significantly increased in OE-*AabZIP1* and decreased in RNAi-*AabZIP1* lines (Fig. 4B and Fig. S4B), respectively. The effect of *AabZIP1* on the transcriptional activity of *AaDBR2* and *AaALDH1* promoters was further evaluated in tobacco leaves by dual-LUC assays. As expected, the transcriptional activity of *AaDBR2* and *AaALDH1* promoters were enhanced by *AabZIP1*, and their activities are increased by 3.5- and 6.7-fold, respectively (Fig. 4C and D).

As revealed by sequence analysis, there are four ABRE *cis*-elements in *AaDBR2* and two in *AaALDH1* promoters (Fig. 4E and F). The fragments containing these individual ABRE *cis*-elements were separately inserted into pLacZ vectors for Y1H assays. Unexpectedly, Y1H results indicated *AabZIP1* did not bind to any of the ABRE *cis*-elements from *AaDBR2* and *AaALDH1* promoters (Fig. 4G and H). Based on these results, we infer that the regulatory mode in which *AabZIP1* upregulates *AaDBR2* and *AaALDH1* expression may be different from how it regulates *AaADS* and *AaCYP71AV1*<sup>36</sup> or the wax biosynthesis genes *AaCER1* and *AaCYP86A1*.

*AaMYC2* is a key JA responsive TF that has been shown to regulate artemisinin biosynthesis<sup>38</sup>. *AaMYC2* is known to be transcriptionally induced by ABA<sup>38</sup>; furthermore, previous studies<sup>36</sup> and our data given by Y1H and Dual-LUC revealed that *AabZIP1* indirectly upregulated the expression of *AaDBR2*, and *AaDBR2* was directly transactivated by *AaMYC2*<sup>38</sup>. These results suggested *AaMYC2* might be a regulating target of *AabZIP1*, the key ABA-responsive TF in *A. annua*<sup>36</sup>. So it is interesting whether *AaMYC2* is regulated by *AabZIP1*. Then, the promoter sequence of *AaMYC2* was isolated and analyzed, and four ABRE *cis*-elements in *AaMYC2* promoter were identified through promoter prediction software (Supporting Information Fig. S5). It was found that OE-*AabZIP1* transgenic lines exhibited 3.1–5.1-fold higher expression level of *AaMYC2* compared to the wild-type by qRT-PCR (Fig. 5A). By contrast, the transcript levels of *AaMYC2* were significantly suppressed in RNAi-*AabZIP1* lines (Fig. S4A). These results prompted us to hypothesize that *AabZIP1* may be the transactivator of *AaMYC2*, which would in turn activate the expression of *AaDBR2* and *AaALDH1*. Dual-LUC assays in tobacco leaves showed that the transcriptional activity of *AaMYC2* promoter was activated by *AabZIP1*, resulting in an increase of 3.7-fold compared with the control (Fig. 5B and C). Y1H results showed that *AabZIP1* could directly bind to the pAaMYC2-R2 fragment but not the other three ABRE motifs in the *AaMYC2* promoter, and that the mutations in the R2 element (pAaMYC2-mR2) abolished the binding of *AabZIP1* (Fig. 5D and E). The EMSA assay further confirmed that *AabZIP1* could specifically bind to the ABRE *cis*-element of pAaMYC2-R2 *in vitro* (Fig. 5F). Together these results indicate that *AabZIP1* directly activates the transcription of *AaMYC2* by binding to its promoter.

It has been reported that *AaMYC2* upregulates the expression of *AaCYP71AV1* and *AaDBR2* by binding to their promoters, thus promoting artemisinin biosynthesis. Although the expression of *AaADS* and *AaALDH1* are also markedly increased in *AaMYC2*-overexpressing *A. annua* lines<sup>38</sup>, how these genes are regulated by *AaMYC2* is unclear. Herein, Dual-LUC assays were used to investigate the mechanism of how *AaMYC2* regulated the expression of *AaADS* and *AaALDH1*. The effectors (35S:YFP or 35S:*AaMYC2*) along with the reporters (pAaADS:LUC and pAaALDH1:LUC) (Fig. 6A) were transiently co-expressed in the *N. benthamiana* leaf cells. The results showed that *AaMYC2*

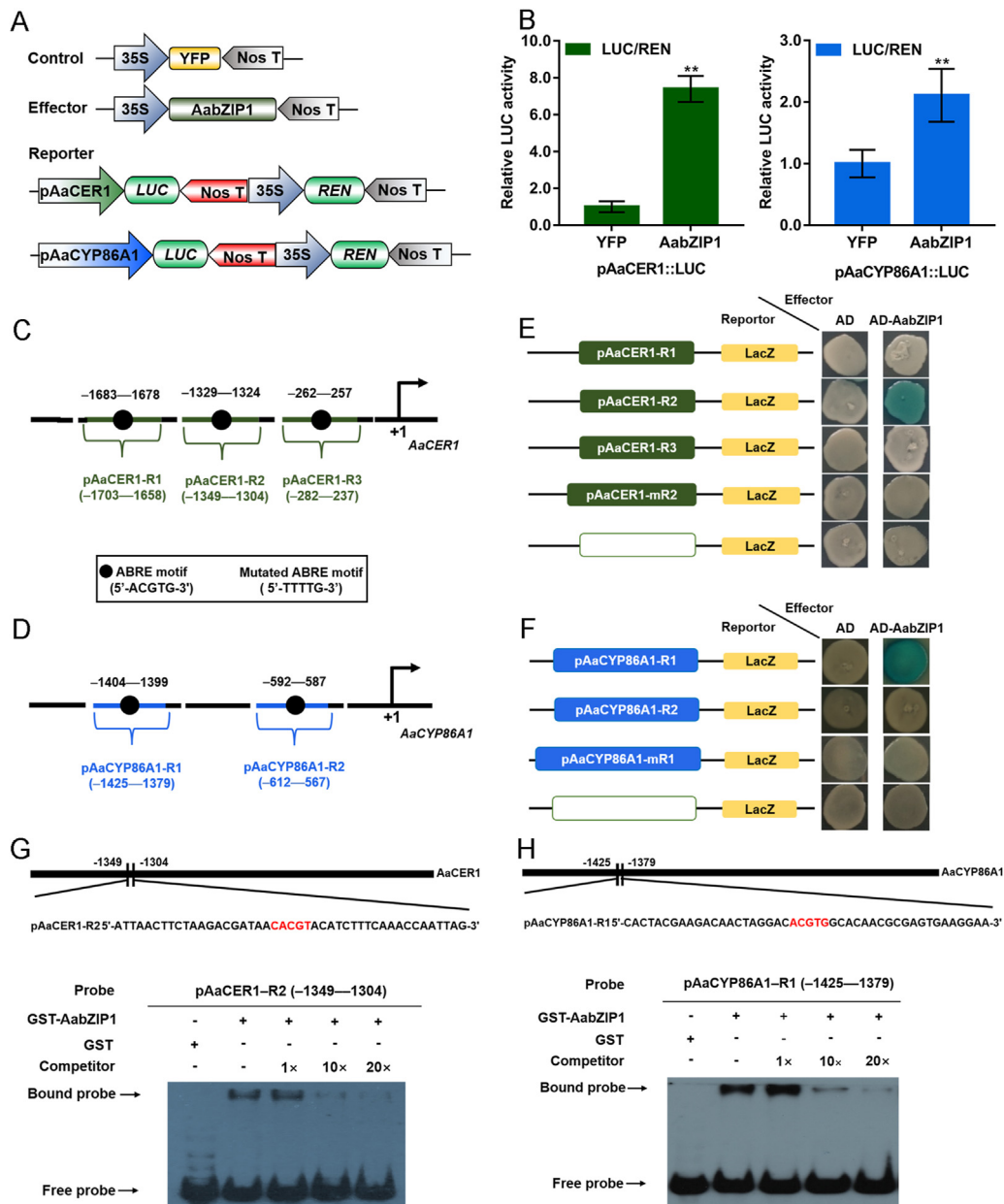


**Figure 3** AabZIP1 is a transcriptional activator of wax biosynthesis gene *AaCER1* and *AaCYP86A1*. (A) Diagrams of reporter and effector constructs in transient dual-luciferase assays (REN, renilla luciferase; LUC, firefly luciferase). (B) Effects of AabZIP1 on activities of the *AaCER1* and *AaCYP86A1* promoters in *N. benthamiana* cells using the constructs shown in (A). The YFP effector was used as a negative control, and the LUC/REN ratios of YFP were set as 1. The data represents the means  $\pm$  SD ( $n = 3$ ),  $**P < 0.01$  in Student's *t*-test. (C–D) Schematic diagrams of the *AaCER1* (C) and *AaCYP86A1* (D) promoters. The positions of potential ABA-responsive elements (ABRE, bZIP binding site) are shown as black circles and are numbered based on their distance from the translational start site (ATG), which is set as +1. (E–F) Y1H assay showing that AabZIP1 binds to the pAaCER1-R2 and pAaCYP86A1-R1 of the *AaCER1* and *AaCYP86A1* promoters, respectively. The ABRE (ACGTG) motifs in the pAaCER1-R2 and pAaCYP86A1-R1 fragments were mutated to the TTTTG sequences resulting in pAaCER1-mR2 and pAaCYP86A1-mR1, respectively. Blue plaques indicate protein-DNA interactions. The Y1H assays were repeated three times, and representative results are shown. (G–H) EMSA assays showing that AabZIP1 binds to the pAaCER1-R2 and pAaCYP86A1-R1 sequences from *AaCER1* and *AaCYP86A1* promoters, respectively. The GST-AabZIP1 fusion protein and labeled probe were used. The GST protein was used as a negative control. Unlabeled pAaCER1-R2 and pAaCYP86A1-R1 sequences were used as the competitor DNA at molar ratios of 1 $\times$ , 10 $\times$  and 20 $\times$ .

activated the transcriptional activity of *AaALDH1* promoter, but not the *AaADS* promoter in tobacco leaves (Fig. 6B and C). Correspondingly, Y1H assays showed AaMYC2 was able to specifically bind to the G-box motif of pAaALDH1-G2 fragment from the *AaALDH1* promoter (Fig. 6G), but was unable to bind to

the G-box-containing pAaADS-G1 and pAaADS-G2 fragments from the *AaADS* promoter in yeast cells (Fig. 6F). The EMSA assay further confirmed that AaMYC2 could specifically bind to the G-box motif of pAaALDH1-G2 *in vitro* (Fig. 6H). These results strongly suggest that *AaALDH1* is also a direct

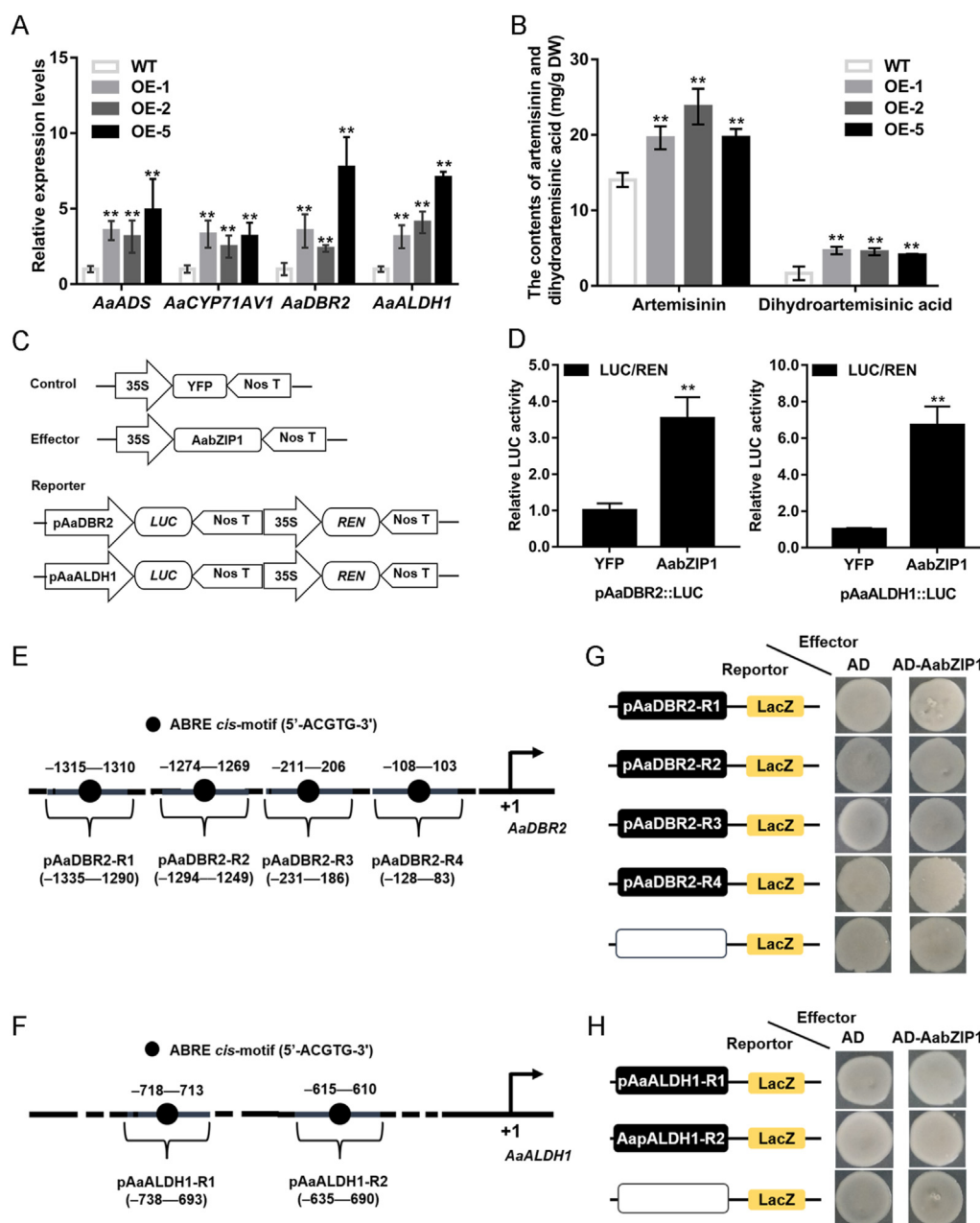


**Figure 4** AabZIP1 transgenic plants modulate artemisinin biosynthesis. (A) Expression levels of *AaADS*, *AaCYP71AV1*, *AaDDBR2*, and *AaALDH1* in the leaves of different *A. annua* AabZIP1-overexpressing (OE-AabZIP1) and wild-type (WT) plants. *AaActin* was used as the internal control. (B) Contents of artemisinin and dihydroartemisinic acid contents in the leaves of different *A. annua* OE-AabZIP1 and WT plants. OE-1, OE-2 and OE-5 are independent lines of AabZIP1-overexpressing *A. annua* plants. All data represents the means  $\pm$  SD ( $n = 3$ ),  $**P < 0.01$  in Student's *t*-test. (C) Diagrams of reporter and effector constructs in transient dual-luciferase assays (REN, renilla luciferase; LUC, firefly luciferase). (D) Effects of AabZIP1 on activities of the *AaDDBR2* and *AaALDH1* promoters in *N. benthamiana* cells using the constructs shown in (C). The YFP effector was used as a negative control, and the LUC/REN ratios of YFP were set as 1. The data represents the means  $\pm$  SD of three replicates from three independent experiments. (E–F) Schematic diagrams of the *AaDDBR2* (E) and *AaALDH1* (F) promoters. The positions of potential ABA-responsive elements (ABRE, bZIP binding site) are shown as black circles and are numbered based on their distance from the translational start site (ATG), which is set as +1. (G–H) Y1H assay showing that AabZIP1 cannot bind to any of the ABRE motifs from *AaDDBR2* (G) and *AaALDH1* (H) promoters.

transcriptional target of AaMYC2, in addition to *AaCYP71AV1* and *AaDDBR2*. Taken together, the above results indicate that AabZIP1 could directly activate the transcription of AaMYC2 by binding to its promoter, thus enhancing the expression of artemisinin biosynthesis genes.

#### 4. Discussion

Our study reported that AabZIP1 plays a dual role in response to drought: enhancing wax production to tolerate drought conditions, and increasing artemisinin biosynthesis. We have identified

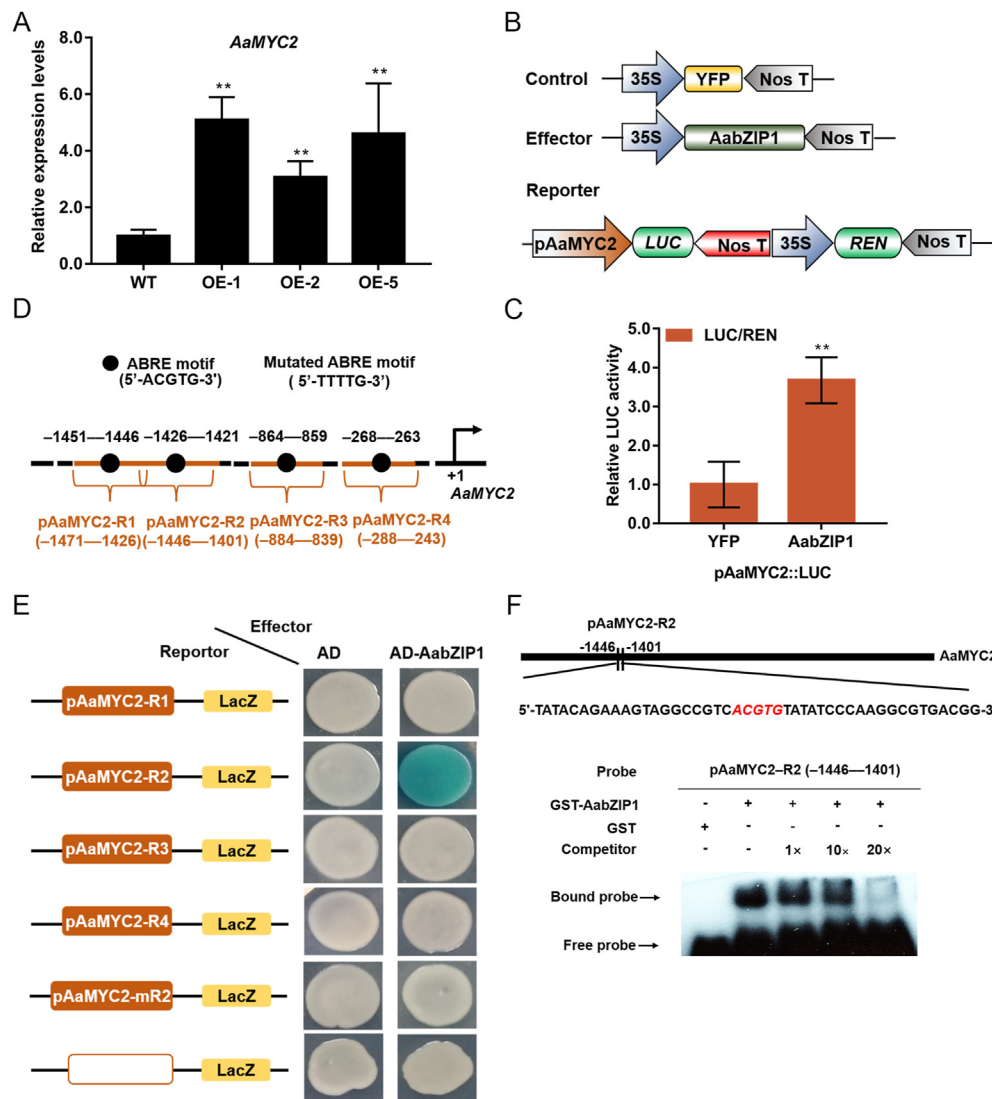


**Figure 5** AabZIP1 directly and positively regulates the expression of *AaMYC2*. (A) Expression levels of *AaMYC2* in the leaves of different *A. annua* *AabZIP1*-overexpressing (OE-*AabZIP1*) and wild-type (WT) plants. OE-1, OE-2 and OE-5 are independent lines of *AabZIP1*-overexpressing *A. annua* plants. *AaActin* was used as the internal control. The data represents the means  $\pm$  SD ( $n = 3$ ),  $**P < 0.01$  in Student's *t*-test. (B) Diagrams of reporter and effector constructs in transient dual-luciferase assays (REN, renilla luciferase; LUC, firefly luciferase). (C) Effects of *AabZIP1* on activities of the *AaMYC2* promoter in *N. benthamiana* cells using the constructs shown in (B). The YFP effector was used as a negative control, and the LUC/REN ratios of YFP were set as 1. The data represents the means  $\pm$  SD ( $n = 3$ ). (D) Schematic diagrams of the *AaMYC2* promoter. The positions of potential ABA-responsive elements (ABRE, bZIP binding site) are shown as black circles and are numbered based on their distance from the translational start site (ATG), which is set as +1. (E) Y1H assay showing that *AabZIP1* binds to the pAaMYC2-R2 of the *AaMYC2* promoter. The ABRE (ACGTG) motifs in the pAaMYC2-R2 fragment were mutated to the TTTTG sequences resulting in pAaMYC2-mR2. Blue plaques indicate protein-DNA interactions. The Y1H assays were repeated three times, and representative results are shown. (F) EMSA assays showing that *AabZIP1* binds to the pAaMYC2-R2 sequence from *AaMYC2* promoter. The GST-*AabZIP1* fusion protein and labeled probe were used. The GST protein was used as a negative control. Unlabeled pAaMYC2-R2 sequence was used as the competitor DNA at molar ratios of 1 $\times$ ; 10 $\times$  and 20 $\times$ .

several new transcriptional targets of *AabZIP1* in these two pathways. In particular, *AabZIP1* is capable of directly binding to *AaMYC2* promoter and stimulating its transcription, thereby activating the JA pathway to coordinate the artemisinin production. This finding identifies *AabZIP1* as a key player in mediating the cross talk between ABA and JA pathways in *A. annua*. It remains to be seen whether ABF1, the *Arabidopsis* homolog to *AabZIP1* plays a similar role in ABA-JA cross-talk in *Arabidopsis* and what physiological consequences it may cause.

#### 4.1. *AabZIP1* improves drought resistance of *A. annua* by promoting cuticular wax biosynthesis

While interacting with the external environment, plants respond to stress cues through various regulatory mechanisms to help them better cope with the stress. The accumulation of cuticular wax across the surface of plant organs is an important strategy for plants to reduce non-stomata water loss<sup>17</sup>. The expression of wax biosynthesis genes and cuticular wax content are increased

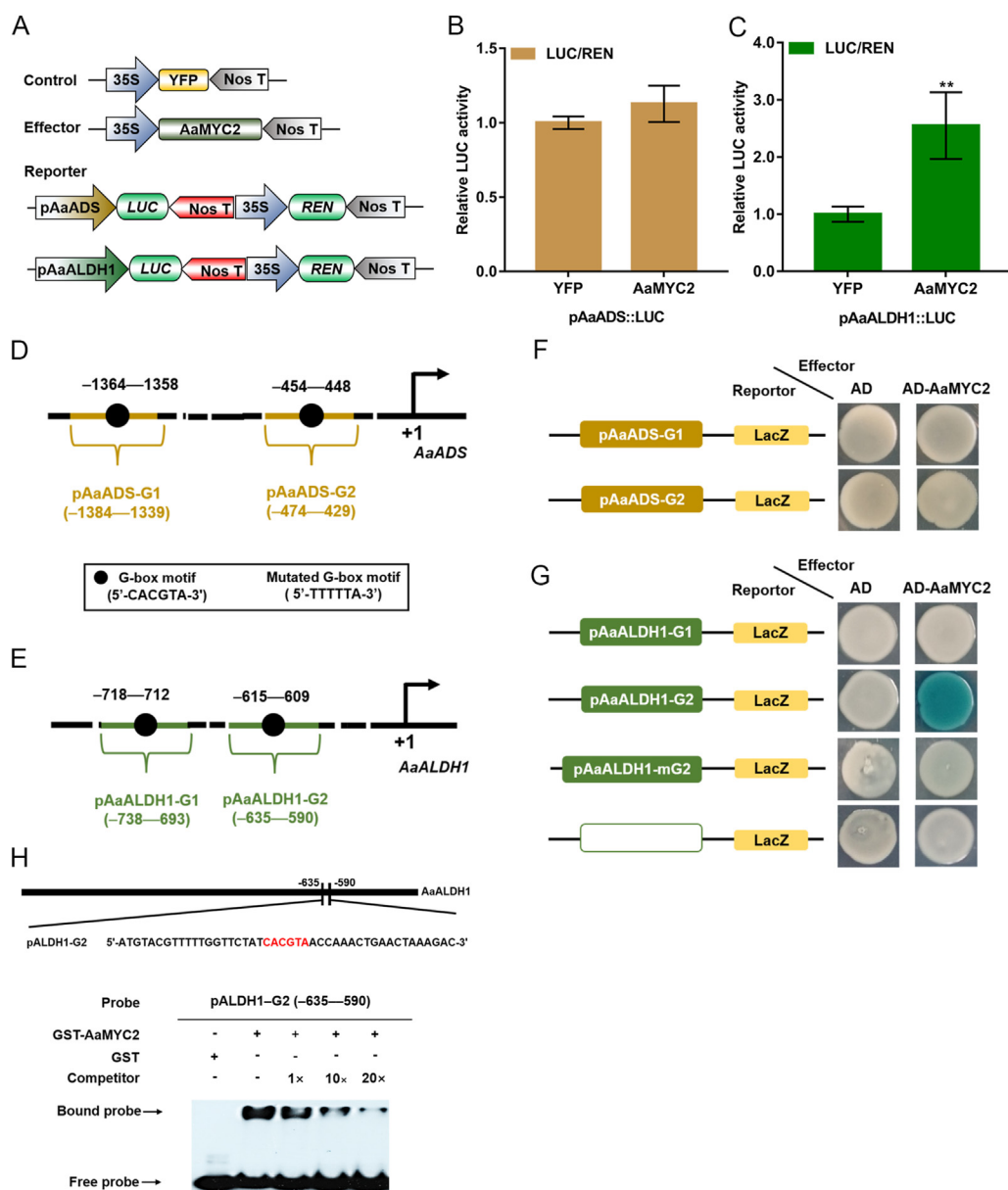


**Figure 6** AaMYC2 directly and positively activates the transcription of *AaALDH1* rather than *AaADS*. (A) Diagrams of reporter and effector constructs in transient dual-luciferase assays (REN, renilla luciferase; LUC, firefly luciferase). (B–C) Effects of AaMYC2 on activities of the *AaADS* and *AaALDH1* promoters in *N. benthamiana* cells using the constructs shown in (A). The YFP effector was used as a negative control, and the LUC/REN ratios of YFP were set as 1, the data represents the means  $\pm$  SD ( $n = 3$ ),  $**P < 0.01$  in Student's *t*-test. (D–E) Schematic diagrams of the *AaADS* and *AaALDH1* promoters. The positions of potential G-box elements (MYC binding site) are shown as black circles and are numbered based on their distance from the translational start site (ATG), which is set as +1. (F–G) Y1H assay showed that AaMYC2 binds to the pAaALDH1-G2 of the *AaALDH1* promoter. The G-box (CACGTA) motifs in the pAaALDH1-G2 fragment were mutated to the TTTTAA sequences resulting in pAaALDH1-mG2. Blue plaques indicate protein-DNA interactions. The Y1H assays were repeated three times, and representative results are shown. (H) EMSA assays showing that AaMYC2 binds to the pAaALDH1-G2 sequence from *AaALDH1* promoter. The GST-AaMYC2 fusion protein and labeled probe were used. The GST protein was used as a negative control. Unlabeled pAaMYC2-R2 sequence was used as the competitor DNA at molar ratios of 1 $\times$ ; 10 $\times$  and 20 $\times$ .

markedly under drought stress in order to prevent water loss<sup>23</sup>. In *A. annua*, *AaCER1*, *AaCYP86A1*, *AaKCS5* and *AaFDH* are closely correlated with wax biosynthesis<sup>30,31</sup>, but the connection between these wax-related genes and drought stress is far from clear. The expression of *AtCER1* and *AtKCS* were induced by drought stress in *Arabidopsis thaliana*<sup>16,46</sup>. Similarly, we found that the expression of multiple wax biosynthesis genes (*AaCER1*, *AaKCS5* and *AaCYP86A1*) in wild type *A. annua*

were significantly up-regulated under drought stress at a slower rate than that the induction of *AabZIP1* (Fig. 1). However, the expression of *AaFDH* was not induced by drought stress (Supporting Information Fig. S6). This was not unexpected, given the complexity for wax component involved in drought response<sup>47</sup>.

The ABA signaling is induced in the response of plants to drought stress<sup>48,49</sup>. Similarly, we found that the expression levels of *AaCER1*

and *AaCYP86A1* were markedly up-regulated under ABA treatment (Fig. 1). In *Arabidopsis*, a number of TFs, such as the AP2/EREBP, MYB, and WRKY types, have been implicated in wax biosynthesis in response to drought<sup>26,50</sup>. In ABA-induced genes expression analysis, we noted that the time points of the highest expression of *AabZIP1* occurred earlier than those of *AaCER1* and *AaCYP86A1*, which indicated that *AabZIP1* has the potential to regulate the expression of *AaCER1* and *AaCYP86A1*. Indeed, *AabZIP1* can recognize and bind to the specific ABRE motifs in the promoters of *AaCER1* and *AaCYP86A1*, and activate their gene expression (Fig. 3). This conclusion is further supported by the *AabZIP1* over-expression studies, as the expression of *AaCER1* and *AaCYP86A1* were significantly up-regulated, and the accumulations of cuticular wax compounds, including alkanes, fatty acids and alcohols, increased markedly in OE-*AabZIP1* transgenic lines. OE-*AabZIP1* lines showed stronger drought tolerance than the wild-type plants (Fig. 2), which was probably resulted from increased cuticle wax biosynthesis and wax deposition on the leaf surface. Meanwhile, the results given by suppression of *AabZIP1* also supported the above conclusion. Our findings identify *AabZIP1* as, to our knowledge, the first bZIP TF that directly binds and targets cuticle wax biosynthesis genes and confers drought tolerance in plants.

#### 4.2. *AabZIP1* promotes artemisinin biosynthesis in part by stimulating the expression of JA responsive transcription factor *AaMYC2*

Artemisinin and its derivatives can rapidly kill Plasmodium parasites, thereby effectively treating malaria, but the current production of artemisinin is insufficient to meet the global

demand. Previous research has shown that ABA enhances artemisinin content by promoting the expression of four key enzyme genes, *AaADS*, *AaCYP71AV1*, *AaDBR2* and *AaALDH1*, involved in artemisinin biosynthesis<sup>51</sup>, but our understanding on the mechanisms of their gene regulation is incomplete. TFs play important roles in plants by controlling the expression of genes involved in secondary metabolic pathways<sup>52</sup>. *AabZIP1* is a critical regulator of ABA-induced artemisinin biosynthesis<sup>36,53</sup>. Herein, we found that the expression levels of artemisinin biosynthesis genes, *AaADS*, *AaCYP71AV1*, *AaDBR2* and *AaALDH1*, were all significantly increased in OE-*AabZIP1* and decreased in RNAi-*AabZIP1* lines (Fig. 4 and Fig. S4), respectively. However, the exact mechanism by which *AabZIP1* regulates these genes is different.

Previous research showed that *AabZIP1* directly regulates the transcription of *AaADS* and *AaCYP71AV1* by binding to the ABRE *cis*-elements on their promoters<sup>36</sup>. In this study, we found that *AabZIP1* does not bind to the ABRE *cis*-elements on *AaDBR2* and *AaALDH1* promoters (Fig. 4), which indicates that *AabZIP1* upregulates *AaDBR2* and *AaALDH1* expression may be different from how it regulates *AaADS* and *AaCYP71AV1*. It is possible that the flanking sequences near ABRE *cis*-element on *AaDBR2* and *AaALDH1* promoters are not optimal for TF binding, and therefore *AabZIP1* could not directly activate their expression.

Beside *AabZIP1*, the JA signaling master transcription factor *AaMYC2* also plays a key role in promoting ABA- and JA-induced artemisinin biosynthesis, and it acts in part by directly regulating the expression of *AaCYP71AV1* and *AaDBR2* on their promoters<sup>38</sup>. MYC2 is an integrator and regulator for ABA and JA signaling pathways in plants. The induction of *AaMYC2* by ABA

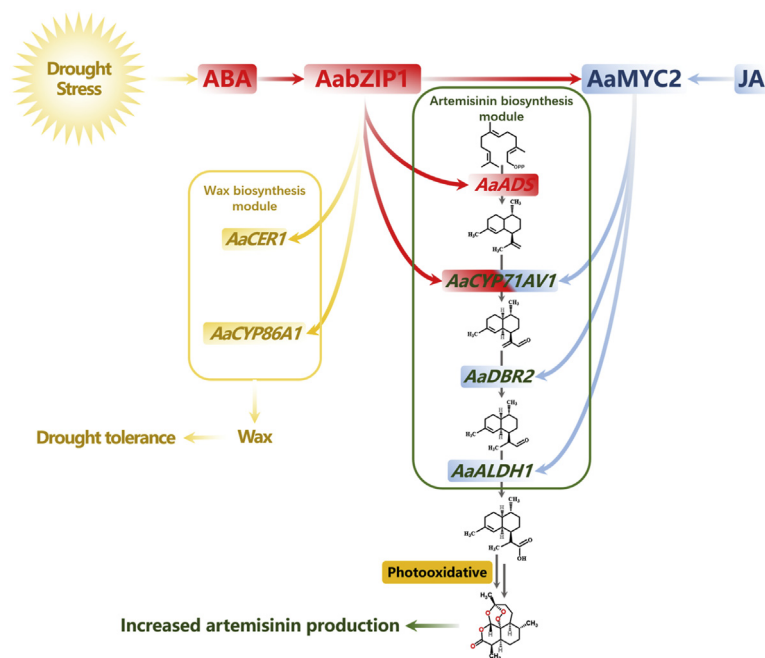


**Figure 7** Proposed working model illustrating how the *AabZIP1* enhances drought resistance and regulates artemisinin biosynthesis in response to ABA signaling. *AabZIP1* and *AaMYC2* TFs are positive regulators of artemisinin biosynthesis, which are positively activated by ABA or JA<sup>36,38</sup>. *AabZIP1* can bind to and activates the *AaADS* and *AaCYP71AV1* promoters<sup>36</sup>. *AaMYC2* promotes artemisinin biosynthesis by positively regulating *AaCYP71AV1* and *AaDBR2* transcription<sup>38</sup>, and *AaMYC2* directly activate the expression of *AaALDH1*. *AabZIP1* and *AaMYC2* directly activate the expression of their common target gene *AaCYP71AV1*. Meanwhile, *AabZIP1* can activate the expression of *AaDBR2* and *AaALDH1* indirectly via *AaMYC2* to promote artemisinin production. In addition, the transcription of *AabZIP1* is positively activated by drought stress and ABA, and *AabZIP1* can directly transactivate *AaCER1* and *AaCYP86A1* to promote cuticular wax biosynthesis, which would contribute to the enhanced drought tolerance in the OE-*AabZIP1* transgenic *A. annua* plants.

represents an important point of cross-talk between ABA and JA signaling, but the mechanism of its transcriptional induction is unknown in *A. annua*. Here, we found that AabZIP1 can directly activate the transcription of AaMYC2 by binding to its promoter (Fig. 5), resulting in the stimulation AaMYC2 regulatory module of the JA pathway. AaMYC2 in turn directly activates the transcription of AaALDH1 as part of its function in regulating artemisinin biosynthesis (Fig. 6). Taken together, these results showed that AabZIP1 regulates artemisinin biosynthesis both directly by targeting the transcription of AaADS and AaCYP71AV1<sup>36</sup>, and indirectly regulates the transcription of AaCYP71AV1, AaDBR2 and AaALDH1 via AaMYC2 (Fig. 7). In an apparently parallel pathway, AabZIP1 has also been shown to promote AaDBR2 and AaALDH1 expression by regulating the transcription of AaTCP14 and AaTCP15<sup>54,55</sup>. It seems that both the AabZIP-AaMYC2 pathway or the AabZIP1-AaTCP14/15 pathway may result in the activation of AaDBR2 and AaALDH1. The relationship and circumstances of these two pathways remain to be investigated. In view of the fact that the expression of AaMYC2 was up-regulated after ABA treatment<sup>38</sup>, our study uncovered the AabZIP1-AaMYC2-CYP71AV1/DBR2/ALDH1 transcriptional regulatory module that is activated by ABA and connected to the JA pathway, enabling the AaMYC2-mediated transcription network part of the ABA responses in artemisinin biosynthesis. While this study revealed that AabZIP1 activation of AaMYC2 is a key point of the cross-talk in the ABA and JA signaling pathways involving artemisinin biosynthesis, it reasonable to suggest that the bZIP-MYC2 transcriptional module may have a general role in the ABA-JA signaling cross-talk in other plants or physiological responses.

## 5. Conclusions

In this study, it was found that AabZIP1 up-regulates AaMYC2 expression through direct binding to its promoter, and AaMYC2 binds to the promoter of AaALDH1 to activate its transcription, suggesting that AabZIP1 could positively regulates the transcription of artemisinin biosynthesis genes indirectly via AaMYC2. In addition, in response to drought stress or ABA, AabZIP1 transcriptionally activates wax biosynthesis genes to promote the accumulation of cuticular wax, resulting in enhanced drought tolerance in *A. annua*. Taken together previous knowledge and results from this study, we illustrate the roles of AabZIP1 in regulating artemisinin biosynthesis and wax biosynthesis in response to drought stress (Fig. 7).

## Acknowledgments

This research was financially supported by the NSFC project (81973420 and 81803660), the National Key Research and Development Project (2019YFE0108700, China), the Natural Science Foundation of Chongqing (cstc2018jcyjAX0328, China) and the Science Funding of Sichuan Province (2020YJ0171, China).

## Author contributions

Zhihua Liao conceived and designed the entire research plans. Guoping Shu performed most of the experiments; Min Chen, Kexuan Tang and Xiaozhong Lan provided resources for detection. Mingyuan Yuan and Chunxian Yang managed the plant materials. Guoping Shu, Fangyuan Zhang and Lien Xiang

analyzed the data. Zhihua Liao, Yueli Tang, Ning Wei and Guoping Shu wrote the article.

## Conflicts of interest

The authors declare no conflict of interest.

## Appendix A. Supporting information

Supporting information to this article can be found online at <https://doi.org/10.1016/j.apsb.2021.09.026>.

## References

1. Tu Y. The discovery of artemisinin (qinghaosu) and gifts from Chinese medicine. *Nat Med* 2011;**17**:1217–220.
2. Li J, Casteels T, Frogne T, Ingvorsen C, Honoré C, Courtney M, et al. Artemisinins target GABA<sub>A</sub> receptor signaling and impair  $\alpha$  cell identity. *Cell* 2017;**168**:86–100.
3. Miller MJ, Walz AJ, Zhu H, Wu C, Moraski G, Möllmann U, et al. Design, synthesis, and study of a mycobactin–artemisinin conjugate that has selective and potent activity against tuberculosis and malaria. *J Am Chem Soc* 2011;**133**:2076–9.
4. Tran KQ, Tin AS, Firestone GL. Artemisinin triggers a G1 cell cycle arrest of human Ishikawa endometrial cancer cells and inhibits cyclin-dependent kinase-4 promoter activity and expression by disrupting nuclear factor- $\kappa$ B transcriptional signaling. *Anti-Cancer Drugs* 2014;**25**:270–81.
5. Ro DK, Paradise EM, Ouellet M, Fisher KJ, Newman KL, Ndungu JM, et al. Production of the antimalarial drug precursor artemisinic acid in engineered yeast. *Nature* 2006;**440**:940–3.
6. Westfall PJ, Pitera DJ, Lenihan JR, Eng D, Woolard FX, Regentin R, et al. Production of amorpha-4,11-diene in yeast, and its conversion to dihydroartemisinic acid, precursor to the antimalarial agent artemisinin. *Proc Natl Acad Sci U S A* 2012;**109**:111–8.
7. Graham IA, Besser K, Blumer S, Branigan CA, Czechowski T, Elias L, et al. The genetic map of *Artemisia annua* L. identifies loci affecting yield of the antimalarial drug artemisinin. *Science* 2010;**327**:328–31.
8. Lesk C, Rowhani P, Ramankutty N. Influence of extreme weather disasters on global crop production. *Nature* 2016;**529**:84–7.
9. Tabassum T, Farooq M, Ahmad R, Zohaib A, Wahid A. Seed priming and transgenerational drought memory improves tolerance against salt stress in bread wheat. *Plant Physiol Biochem* 2017;**118**:362–9.
10. Selvaraj MG, Ishizaki T, Valencia M, Ogawa S, Dedicova B, Ogata T, et al. Overexpression of an *Arabidopsis thaliana* galactinol synthase gene improves drought tolerance in transgenic rice and increased grain yield in the field. *Plant Biotechnol J* 2017;**15**:1465–77.
11. Zhang X, Lei L, Lai J, Zhao H, Song W. Effects of drought stress and water recovery on physiological responses and gene expression in maize seedlings. *BMC Plant Biol* 2018;**18**:68.
12. Yadav RK, Sangwan RS, Sabir F, Srivastava AK, Sangwan NS. Effect of prolonged water stress on specialized secondary metabolites, peltate glandular trichomes, and pathway gene expression in *Artemisia annua* L. *Plant Physiol Biochem* 2014;**74**:70–83.
13. Vashisth D, Kumar R, Rastogi S, Patel VK, Kalra A, Gupta MM, et al. Transcriptome changes induced by abiotic stresses in *Artemisia annua*. *Sci Rep* 2018;**8**:3423.
14. Obata T, Fernie AR. The use of metabolomics to dissect plant responses to abiotic stresses. *Cell Mol Life Sci* 2012;**69**:3225–43.
15. Li RJ, Li LM, Liu XL, Kim JC, Jenks MA, Lü S. Diurnal regulation of plant epidermal wax synthesis through antagonistic roles of the transcription factors SPL9 and DEWAX. *Plant Cell* 2019;**31**:2711–33.
16. Seo PJ, Park CM. Cuticular wax biosynthesis as a way of inducing drought resistance. *Plant Signal Behav* 2011;**6**:1043–5.

17. Dimopoulos N, Tindjau R, Wong DCJ, Matzat T, Haslam T, Song C, et al. Drought stress modulates cuticular wax composition of the grape berry. *J Exp Bot* 2020;**71**:3126–41.
18. Kunst L, Samuels AL. Biosynthesis and secretion of plant cuticular wax. *Prog Lipid Res* 2003;**42**:51–80.
19. Lee SB, Suh MC. Recent advances in cuticular wax biosynthesis and its regulation in *Arabidopsis*. *Mol Plant* 2013;**6**:246–9.
20. Yang X, Feng T, Li S, Zhao H, Zhao S, Ma C, et al. *CER16* inhibits post-transcriptional gene silencing of *CER3* to regulate alkane biosynthesis. *Plant Physiol* 2020;**182**:1211–21.
21. Haslam TM, Kunst L. Extending the story of very-long-chain fatty acid elongation. *Plant Sci* 2013;**210**:93–107.
22. Yephremov A, Wisman E, Huijser P, Huijser C, Wellesen K, Saedler H. Characterization of the FIDDLEHEAD gene of *Arabidopsis* reveals a link between adhesion response and cell differentiation in the epidermis. *Plant Cell* 1999;**11**:2187–201.
23. Aharoni A, Dixit S, Jetter R, Thoenes E, Van AG, Pereira A. The SHINE clade of AP2 domain transcription factors activates wax biosynthesis, alters cuticle properties, and confers drought tolerance when overexpressed in *Arabidopsis*. *Plant Cell* 2004;**16**:2463–80.
24. Zhang JY, Broeckling CD, Blancaflor EB, Sledge MK, Sumner LW, Wang ZY. Overexpression of WXP1, a putative Medicago truncatula AP2 domain-containing transcription factor gene, increases cuticular wax accumulation and enhances drought tolerance in transgenic alfalfa (*Medicago sativa*). *Plant J* 2005;**42**:689–707.
25. Howell SH. Endoplasmic reticulum stress responses in plants. *Annu Rev Plant Biol* 2013;**64**:477–99.
26. Lee SB, Kim HU, Suh MC. MYB94 and MYB96 additively activate cuticular wax biosynthesis in *Arabidopsis*. *Plant Cell Physiol* 2016;**57**:2300–11.
27. Yang SU, Kim H, Kim RJ, Kim J, Suh MC. AP2/DREB transcription factor RAP2.4 activates cuticular wax biosynthesis in *Arabidopsis* leaves under drought. *Front Plant Sci* 2020;**11**:895.
28. Xiong C, Xie Q, Yang Q, Sun P, Gao S, Li H, et al. WOOLLY, interacting with MYB transcription factor MYB31, regulates cuticular wax biosynthesis by modulating CER6 expression in tomato. *Plant J* 2020;**103**:323–37.
29. Tan H, Xiao L, Gao S, Li Q, Chen J, Xiao Y, et al. TRICHOME AND ARTEMISININ REGULATOR 1 is required for trichome development and artemisinin biosynthesis in *Artemisia annua*. *Mol Plant* 2015;**8**:1396–411.
30. Shi P, Fu X, Shen Q, Liu M, Pan Q, Tang Y, et al. The roles of AaMIXTA1 in regulating the initiation of glandular trichomes and cuticle biosynthesis in *Artemisia annua*. *New Phytol* 2017;**217**:261–76.
31. Yan T, Li L, Xie L, Chen M, Shen Q, Pan Q, et al. A novel HD-ZIP IV/MIXTA complex promotes glandular trichome initiation and cuticle development in *Artemisia annua*. *New Phytol* 2018;**218**:567–78.
32. Xiang Y, Tang N, Du H, Ye H, Xiong L. Characterization of OsbZIP23 as a key player of the basic leucine zipper transcription factor family for conferring abscisic acid sensitivity and salinity and drought tolerance in rice. *Plant Physiol* 2008;**148**:1938–52.
33. An JP, Yao JF, Xu RR, You CX, Wang XF, Hao YJ. Apple bZIP transcription factor MdbZIP44 regulates abscisic acid-promoted anthocyanin accumulation. *Plant Cell Environ* 2018;**41**:2678–92.
34. Deng C, Shi M, Fu R, Zhang Y, Wang Q, Zhou Y, et al. ABA-responsive transcription factor bZIP1 is involved in modulating biosynthesis of phenolic acids and tanshinones in *Salvia miltiorrhiza*. *J Exp Bot* 2020;**71**:5948–62.
35. Zhang Y, Xu Z, Ji A, Luo H, Song J. Genomic survey of bZIP transcription factor genes related to tanshinone biosynthesis in *Salvia miltiorrhiza*. *Acta Pharm Sin B* 2018;**8**:295–305.
36. Zhang F, Fu X, Lv Z, Lu X, Shen Q, Zhang L, et al. A basic leucine zipper transcription factor, AabZIP1, connects abscisic acid signaling with artemisinin biosynthesis in *Artemisia annua*. *Mol Plant* 2015;**8**:163–75.
37. Wang H, Ma C, Li Z, Ma L, Wang H, Ye H, et al. Effects of exogenous methyl jasmonate on artemisinin biosynthesis and secondary metabolites in *Artemisia annua* L. *Ind Crops Prod* 2010;**31**:214–8.
38. Shen Q, Lu X, Yan T, Fu X, Lv Z, Zhang F, et al. The jasmonate-responsive AaMYC2 transcription factor positively regulates artemisinin biosynthesis in *Artemisia annua*. *New Phytol* 2016;**210**:1269–81.
39. Abe H, Yamaguchi-Shinozaki K, Urao T, Iwasaki T, Hosokawa D, Shinozaki K. Role of *arabidopsis* MYC and MYB homologs in drought- and abscisic acid-regulated gene expression. *Plant Cell* 1997;**9**:1859–68.
40. Abe H, Urao T, Ito T, Seki M, Shinozaki K, Yamaguchi-Shinozaki K. *Arabidopsis* AtMYC2 (bHLH) and AtMYB2 (MYB) function as transcriptional activators in abscisic acid signaling. *Plant Cell* 2003;**15**:63–78.
41. Seo PJ, Xiang F, Qiao M, Park JY, Lee YN, Kim SG, et al. The MYB96 transcription factor mediates abscisic acid signaling during drought stress response in *Arabidopsis*. *Plant Physiol* 2009;**151**:275–89.
42. Sakuraba Y, Kim YS, Han SH, Lee BD, Paek NC. The *Arabidopsis* transcription factor NAC016 promotes drought stress responses by repressing AREB1 transcription through a trifurcate feed-forward regulatory loop involving NAP. *Plant Cell* 2015;**27**:1771–87.
43. Wang W, Wang Y, Zhang Q, Qi Y, Guo D. Global characterization of *Artemisia annua* glandular trichome transcriptome using 454 pyrosequencing. *BMC Genomics* 2009;**10**:465.
44. Livak KJ, Schmittgen TD. Analysis of relative gene expression data using real-time quantitative PCR and the  $2^{-\Delta\Delta CT}$  method. *Methods* 2001;**25**:402–8.
45. Xiang L, Jian D, Zhang F, Yang C, Bai G, Lan X, et al. The cold-induced transcription factor bHLH112 promotes artemisinin biosynthesis indirectly via ERF1 in *Artemisia annua*. *J Exp Bot* 2019;**70**:4835–48.
46. Kosma DK, Bourdenx B, Bernard A, Parsons EP, Lü S, Joubès J, et al. The impact of water deficiency on leaf cuticle lipids of *Arabidopsis*. *Plant Physiol* 2009;**151**:1918–29.
47. Kim KS, Park SH, Jenks MA. Changes in leaf cuticular waxes of sesame (*Sesamum indicum* L.) plants exposed to water deficit. *J Plant Physiol* 2007;**164**:1134–43.
48. Yamaguchi-Shinozaki K, Shinozaki K. Transcriptional regulatory networks in cellular responses and tolerance to dehydration and cold stresses. *Annu Rev Plant Biol* 2006;**57**:781–803.
49. Seki M, Umezawa T, Urano K, Shinozaki K. Regulatory metabolic networks in drought stress responses. *Curr Opin Plant Biol* 2007;**10**:296–302.
50. Lee SB, Suh MC. Cuticular wax biosynthesis is up-regulated by the MYB94 transcription factor in *Arabidopsis*. *Plant Cell Physiol* 2015;**56**:48–60.
51. Jing FY, Zhang L, Li MY, Tang YL, Wang YL, Wang YY, et al. Abscisic acid (ABA) treatment increases artemisinin content in *Artemisia annua* by enhancing the expression of genes in artemisinin biosynthetic pathway. *Biologia* 2009;**64**:319–23.
52. Chu Y, Xiao S, Su H, Liao B, Zhang J, Xu J, et al. Genome-wide characterization and analysis of bHLH transcription factors in *Panax ginseng*. *Acta Pharm Sin B* 2018;**8**:666–77.
53. Hassani D, Fu X, Shen Q, Khalid M, Rose JKC, Tang K. Parallel transcriptional regulation of artemisinin and flavonoid biosynthesis. *Trends Plant Sci* 2020;**25**:466–76.
54. Ma YN, Xu DB, Li L, Zhang F, Fu XQ, Shen Q, et al. Jasmonate promotes artemisinin biosynthesis by activating the TCP14-ORA complex in *Artemisia annua*. *Sci Adv* 2018;**4**:eaas9357.
55. Ma YN, Xu DB, Yan X, Wu ZK, Kayani SI, Shen Q, et al. Jasmonate- and abscisic acid-activated AaGSW1-AaTCP15/AaORA transcriptional cascade promotes artemisinin biosynthesis in *Artemisia annua*. *Plant Biotechnol J* 2021;**19**:1412–28.